Circumferential velocities in laminar and turbulent counter-vortex flow

Genrikh Orekhov

State University of Civil Engineering (National Research University)

Abstract. Knowledge of the parameters of fluid movement is essential in the designing and operating various technological processes in various technical applications. These processes play a special role in hydro engineering, where the structures of water works are directly subjected to static and dynamic forces from the side of the water flow. The operation of hydraulic turbines, spillway and water transport systems, and other hydraulic structures is directly connected with understanding the behavior of a fluid in various regimes of movement. This report is devoted to the study of a special type of fluid and gas flow, which is called counter-vortex flow. The report compares the results of the distribution of circumferential velocities with a laminar and turbulent pattern of fluid movement. The results of the laminar flow regime were obtained using a mathematical model, and the turbulent regime on a physical model using laser technologies. Such a comparison allows one to assess two approaches in determining the kinematic structures of a complicated flow. The parameters for the viscous fluid laminar flow were determined based on the traditional system of Navier-Stokes equations by determining the dependence of the circumferential component of the total velocity at the given initial circulations and angular flow velocity. A physical model was made and equipped with a set of measuring equipment to obtain the distribution of velocities in the turbulent flow. The comparison showed that the distributions of velocities for the considered flow regimes depending on the channel radius have close coincidence. In contrast, the transformation length-wise of the active zone of the flow is significant.

1 Introduction

In numerous present-day technological processes, the fluid and gas flows occupy an important place [1, 2, 3]. To a great extent, this applies to hydraulic engineering and hydropower construction. The hydro power facilities include structures that are in direct contact with water flows forming the flow conductor systems of different geometries and made of different materials. The structures interacting with water are subject to dynamic impact from the side of the flow: alternating pressure, vibrations, cavitation and abrasive wear, and others [4, 5, 6]. In hydraulic facilities of various purposes, provision is made for flow conductor systems [7,8,9], which are subdivided into two characteristic types: spillways and water outlets [10, 11, 12, 13]. These structures are intended to pass the flood flow from reservoirs downstream with water levels preset in the design. An integral part of any water conductor system is the flow energy dissipator, which can be of various designs: a stilling well, a jet throw, various ways of swirling the flow [14, 15], and others.

Among the energy dissipation methods of the flow spilled with its swirling, the counter-vortex method stands out, making it possible to effectively dissipate the high-velocity flow energy in a rather short section of the flow conductor [16, 17, 18]. It must be said here that a counter-vortex flow is an artificially created flow in which oppositely swirling layers of fluid or gas interact in a circular cylindrical chamber. Studies on physical models of various scales and in the prototype have shown that 95-98% of the total flow kinetic energy dissipation can occur at a length of up to 10-15 radii of a circular cylindrical tube [19, 20]. In this respect, this method of flow energy dissipation is unique and deserves a detailed study of all parameters of the counter-vortex flow. For several years, work has been carried out to study this type of flow to determine its hydraulic and hydrodynamic characteristics using mathematical, physical modeling, and field tests.

An important characteristic of any flow, including counter-vortex flow, is the distribution of the velocity components over the channel cross-sections and length-wise the flow. This is especially important in the flow under consideration since the flow structure here changes sharply over a relatively short channel length. This report compares the distribution of the axial velocity component obtained theoretically based on the solution of the Navier-Stokes equations and laboratory studies on a physical model by measuring the flow velocity by laser method.

2 Objective

The purpose of this work is to carry out a comparative analysis of the distribution of the circumferential component of the total velocity of the counter-vortex flow in a circular cylindrical tube obtained theoretically and using a physical model by a laser measurement system based on tracer visualization of the flow.

This work aimed to obtain the distributions of the axial velocity component in the area of the active zone of interaction of oppositely rotating layers of the fluid by mathematical and physical modeling methods.

3 Method

Following the set objective, the distribution of the circumferential component of the counter-vortex flow velocity was obtained by an analytical method using the Navier-Stokes equations. Analytical studies, as a rule, in contrast to numerical and physical modeling, allow for describing the physical picture of the phenomenon. Its subsequent analysis provides an opportunity for broad theoretical generalizations. However, this method has exact solutions only in the laminar flow area. This paper gives the results of studies for the Reynolds number equal to 500.

Physical modeling, in contrast to analytical one, allows for studying the flow in a wide range of flows, including the turbulent flow regime, which brings the flow pattern closer to the actual one. The Reynolds numbers at the water conductor systems of water works are rather high, in the range of 10^4-10^7 and higher. In this work, the flow velocities were measured on a model using a PIV laser tracer system in 3D. The diameter of the circular cylindrical channel in which the counter-vortex flow was formed was 200 mm. The *Re* number = 3.8×10^4 .The average flow velocity $V = 2.85$m/s.

4 Results and Discussion

The shape of the counter-vortex flow in the cross-section and coordinates are shown in Figure 1. The study of counter-vortex flows can be carried out by mathematical (analytical or

numerical) and physical methods [21, 22]. This work attempts to investigate it theoretically (analytically) and then compare the results obtained with the measurement data on a physical model.

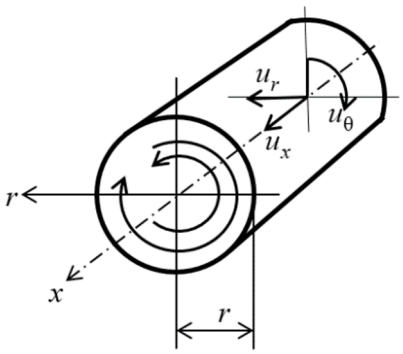

Fig. 1. Counter-vortex flow diagram and coordinate system for circular cylindrical tube

The movement of a steady axisymmetric $\partial / \partial t = 0$ counter-vortex $\partial / \partial \theta = 0$ flow is described by a system of three normalized differential equations with three unknown distributions of the velocity components u_x, u_θ, u_r shown below

$$\left.\begin{aligned} \frac{\partial u_\theta}{\partial x} &= \frac{1}{\mathrm{Re}}\left(\frac{\partial^2 u_\theta}{\partial r^2} + \frac{\partial u_\theta}{r\partial r} - \frac{u_\theta}{r^2}\right), \\ 2\frac{u_\theta}{r}\frac{\partial u_\theta}{\partial x} + \frac{\partial^2 u_x}{\partial x \partial x r} &= \frac{1}{\mathrm{Re}}\frac{\partial}{\partial r}\left(\frac{\partial^2 u_x}{\partial r^2} + \frac{\partial u_x}{r\partial r}\right), \end{aligned}\right\} \quad (1)$$

$$\frac{\partial (r u_r)}{r\partial r} + \frac{\partial u_x}{\partial x} = 0\,. \quad (2)$$

In equations (1) and (2), the independent linear variables (coordinates) are reduced to the flow conductor radius R and the movement velocities are normalized to the average flow velocity of discharge ($V = Q / \pi R^2$). Here u_x, u_θ, u_r are the axial, circumferential, and radial components of the velocity. The Reynolds number is equal to

$$Re = \frac{VR}{\varepsilon}. \quad (3)$$

Let us consider the change in the velocity characteristics of the counter-vortex flow along the radius and length-wise of the tube. Let us take the study area from the initial section, where the oppositely swirling layers come into interaction, to the last section, where the counter-vortex flow completely dies out and turns into a longitudinal-axial and steady-state flow, that is, Poiseuille flow. The counter-vortex flow has two main areas. The area of intensive interaction of swirling layers is called the active zone, and the area where the interaction process of fluid layers ends, and the flow passes into the zone of passive transformation with an uneven axial flow. From the above, the boundary conditions of the problem can be formulated as follows:

- let with $r = 1$, all the velocity components u_r, u_θ, u_x are equal to zero due to the impermeability of the solid flow boundaries and the viscous adhesion of the fluid on the tube walls;
- on the axis of flow rotation (axis of symmetry) with $r = 0$, we set the radial and circumferential velocities $u_r = u_\theta = 0$ to be equal to zero, and for the axial velocities, we set a smooth extremum $\partial u_x / \partial r = 0$;

- at a distance from the inlet section of the counter-vortex flow with $x=\infty$ we accept the soft boundary conditions, according to which the flow is assumed to be uniform. In this case, the radial and circumferential velocities $u_r = u_\theta = 0$ and the particular derivative of the axial velocity along the longitudinal coordinate $\partial u_x / \partial x = 0$ are equal to zero.

Then we have

$$\left.\begin{aligned} &u_r(1,x) = u_\theta(1,x) = u_x(1,x) = 0 \qquad \text{for } 0<x\le\infty, \\ &u_r(0,x) = u_\theta(0,x) = 0, \ \left.\frac{\partial u_x}{\partial r}\right|_{r=0} = 0 \quad \text{for } 0<x\le\infty, \\ &u_r(r,\infty) = u_\theta(r,\infty) = 0, \ \left.\frac{\partial u_x}{\partial r}\right|_{x=\infty} = 0 \quad \text{for } 0\le r\le 1. \end{aligned}\right\} \tag{4}$$

In addition to conditions (4), one should indicate the requirement of maintaining the volumetric flow rate along the cylindrical channel. In normalized form, it is written as equality (5)

$$\int_0^1 u_x 2rdr = 1. \tag{5}$$

With the interaction of the coaxial circulation-longitudinal fluid layers system (1) - (2) with the given boundary conditions (4) - (5) and the known characteristics of swirling fluid layers at the inlet to the active zone Γ_0 and Ω_0 have the solution.

Let us consider the first equation of system (1) - (2). It has a general solution in the form of Fourier-Bessel expansion (6)

$$u_\theta(r,x,\mathrm{Re}) = \sum_{n=1}^{\infty} A_n J_1(\lambda_n r)\exp\left(-\lambda_n^2 \frac{x}{\mathrm{Re}}\right), \tag{6}$$

satisfying the boundary conditions (4). Here λ_n is one of the real roots of the Bessel function of the first kind of the first order $J_n(\lambda_n) = 0$

If the flow swirl system creates the oppositely swirled layers, it forms a counter-vortex flow at the inlet to the active zone (with $x = 0$) corresponding to the profile (7)

$$u_\theta(r,0) = \Omega_0 r + \frac{\Gamma_0}{r}, \tag{7}$$

The final solution of (6) will be the function (8)

$$u_\theta(r,x,\mathrm{Re}) = 2\sum_{n=1}^{\infty} \frac{\Gamma_0\left[1-J_0(\lambda_n)\right]-\Omega_0 J_0(\lambda_n)}{\lambda_n J_0^2(\lambda_n)} J_1(\lambda_n r)\exp(-\lambda_n^2 \frac{x}{\mathrm{Re}}). \tag{8}$$

Here it is necessary to put $\Gamma_0 < 0$, $\Omega_0 > 0$, thus setting the counter-vortex rotation of the coaxial layers. Parameters Γ_0 и Ω_0 are, respectively, the initial circulation and the angular velocity of fluid movement in the tube section with $x = 0$.

Let us assume that the total mutual viscous diffusion of the coaxial layers should correspond to zero of the total angular momentum at the entrance to the active zone ($x = 0$).

$$M\big|_{x=0} = \int_0^1 r u_\theta u_x 2rdr = 0. \tag{9}$$

Here we establish a uniform profile of longitudinal velocities

$$u_x(r,0) = 1. \tag{10}$$

As a result of integrating (9), taking into account (7) and (10), we obtain

$$\Gamma_0 = -\Omega_0 / 2. \tag{11}$$

Condition (11) assumes a flow without residual circulation outside the zone of interaction of liquid layers. As mentioned above, this is a longitudinal-axial flow (Poiseuille flow). Behind the zone of active interaction of oppositely swirling flows, another regime is also possible in which residual mono-circulation is observed. In this case, the flow has a minor circulation of the remaining more powerful peripheral layer or the central one.

An arbitrary radial (transverse) profile of the counter-vortex flow at the inlet to the active zone can be specified by the Taylor power series

$$u_\theta(r,0) = a_1 r + a_2 r^3 + a_3 r^5 + \dots . \tag{12}$$

If the coefficients of the series are set equal

$$a_n = (-1)^{n+1} \frac{(2\pi)^{2n-1}}{(2n-1)!},$$

then we obtain the sinusoidal profile as an inlet one

$$u_\theta(r,0) = \sin(2\pi r),$$

while when the coefficients are set

$$a_n = (-1)^{n+1} \frac{C(C_1)^n}{n!},$$

then the inlet profile of the distribution of the velocities by the radius there will be an eddy corresponding to the expression

$$u_\theta(r,0) = \frac{C}{r}\left[1 - \exp(-C_1 r^2\right]. \tag{13}$$

Thus, the inlet (transversal) profile of the peripheral velocity component can be specified by expression (13). Such a task is possible when applied to a specific practical case being limited by several of its members depending on the required accuracy, after which obtain the desired distribution function of the peripheral velocities formally repeating the operations performed above.

To solve the problem we posed, we proceed as follows. Let us set the configuration of the inlet profile of the counter-vortex flow in the form of the Bessel function. For example, the first kind of the first order (14)

$$u_\theta(r,0) = A_0 J_1(\mu r), \tag{14}$$

where A_0 is arbitrary coefficient; μ is constant not equal to the root of the first-order Bessel function of the first kind of the first order $J_1(\mu) \neq 0$.

To create the conditions for counter-vortex flow, the inequality condition is necessary

$$\mu > \lambda_1,$$

where $\lambda_1 = 3.832$ – the first zero of the Bessel function of the first kind of the first order.

The increase in μ value of more than the second, third, and so on zeros of the Bessel function of the first kind of the first order allows setting the required number of coaxial layers with mutually opposite rotation. This circumstance is an important property of function (14).

If a uniform profile of longitudinal velocities is set at the inlet according to (10), then the flow of angular momentum (9)

$$M\big|_{x=0} = 2A_0 \int_0^1 r^2 J_1(\mu r) dr = 2A_0 \frac{J_2(\mu)}{\mu},$$

will be equal to zero, if μ –is one of the actual roots of the Bessel function of the first kind

of the first order $J_2(\mu) = 0$.

In all other cases, with $J_2(\mu) \neq 0$ the angular moments of flow, the amounts of rotation of the peripheral and inner layers will not equal each other in absolute value. Therefore, the resulting flow outside the active zone must remain circulating-longitudinal ones.

Following (6) and (14) for x = 0 we have

$$A_0 J_1(\mu r) = \sum_{n=1}^{\infty} A_n J_1(\lambda_n r).$$

We multiply the right and left sides of this equality sequentially by $rJ_1(\lambda_1 r)dr$, $rJ_1(\lambda_2 r)dr$, …, $rJ_1(\lambda_n r)dr$, and further to $rJ_1(\lambda_\infty r)dr$, and integrate the products concerning r in the range from 0 to 1. Then, following the orthogonality conditions for the Bessel functions, we obtain a system of equations for relatively constant A_n

$$\left.\begin{aligned}
&A_0 \int_0^1 J_1(\mu r) J_1(\lambda_1 r) r dr = A_1 \int_0^1 J_1(\lambda_1 r) J_1(\lambda_1 r) r dr, \\
&A_0 \int_0^1 J_1(\mu r) J_1(\lambda_2 r) r dr = A_2 \int_0^1 J_1(\lambda_2 r) J_1(\lambda_2 r) r dr, \\
&\ldots \\
&A_0 \int_0^1 J_1(\mu r) J_1(\lambda_n r) r dr = A_n \int_0^1 J_1(\lambda_n r) J_1(\lambda_n r) r dr, \\
&\ldots \\
&A_0 \int_0^1 J_1(\mu r) J_1(\lambda_\infty r) r dr = A_\infty \int_0^1 J_1(\lambda_\infty r) J_1(\lambda_\infty r) r dr.
\end{aligned}\right\}$$

Integrating these equations for an arbitrary n-th special solution, we find

$$A_0 \frac{\lambda_n J_1(\mu) J_0(\lambda_n)}{\mu^2 - \lambda_n^2} = \frac{A_n}{2}\left[J_1'(\lambda_n)\right]^2.$$

With $J_1(\lambda_n) = 0$ we obtain the equation

$$J_0(\lambda_n) = J_1'(\lambda_n),$$

resulting in

$$A_n = \frac{2A_0 J_1(\mu)}{\left[(\mu/\lambda_n)^2 - 1\right]\lambda_n J_0(\lambda_n)}. \tag{15}$$

The product in the numerator of the obtained expression, according to (14), is the normalized peripheral velocity at the wall of a circular tube in the section at the entrance to the active zone of the counter-vortex flow

$$u_\theta(1,0) = A_0 J_1(\mu).$$

This normalized velocity is equal to the Rossby number (*Ro*)

$$u_\theta(1,0) = \frac{u_{\theta 0}}{V} = Ro, \tag{16}$$

where $u_{\theta 0}$ is the peripheral velocity in the near-wall zone at the entrance to the design channel (in this case, at the entrance to the active zone), V is the average flow rate.

We rewrite (15) as

$$A_n = \frac{2Ro}{\left[(\mu/\lambda_n)^2 - 1\right]\lambda_n J_0(\lambda_n)}$$

and substituting this value to (6), we finally obtain (17)

$$u_\theta(r,x,\mathrm{Re}) = 2Ro\sum_{n-1}^{\infty}\frac{J_1(\lambda_n r)}{\left[(\mu/\lambda_n)^2 - 1\right]\lambda_n J_0(\lambda_n)}\exp\left(-\lambda_n^2\frac{x}{\mathrm{Re}}\right). \quad (17)$$

The sum of (8) and (17) will be the general solution of (18)

$$u_\theta(r,x,\mathrm{Re}) = 2\sum_{n-1}^{\infty}G_n\frac{J_1(\lambda_n r)}{\lambda_n J_0(\lambda_n)}\exp\left(-\lambda_n^2\frac{x}{\mathrm{Re}}\right), \quad (18)$$

where λ_n is the root of the Bessel function of the first kind of the first order $J_1(\lambda_n)$, G_n is the constant of the n-th particular solution

$$G_n = \Gamma_0\left[\frac{1}{J_0(\lambda_n)} - 1\right] - \Omega_0 - \frac{Ro^*}{1-(\mu/\lambda_n)^2}, \quad (19)$$

in which μ, Γ_0, Ω_0 Ro^* are the constants depending on the boundary conditions at the entrance to the active zone with μ not equal to the root of the Bessel function of the first kind of the first order $J_1(\mu) \neq 0$.

Let us note that in expression (19) constant

$$Ro^* = A_0 J_1(\mu)$$

does not correspond to the Rossby number (16) because consistent with (7) and (14)

$$u_\theta(1,0) = \Omega_0 + \Gamma_0 + A_0 J_1(\mu),$$

therefore, the real value of the Rossby number by adding three components of the inlet eddy is equal to

$$Ro = \Omega_0 + \Gamma_0 + Ro^*.$$

The change in the configurations of the profiles of the circumferential normalized velocities in the counter-vortex current length-wise flow is shown in Figure 2. These figures show the profiles (diagrams) of the distribution of the circumferential velocity components depending on the radius of the cylindrical channel ($r^* = r/R$) and the distance from the initial section of the active zone. The distances from the inlet section of the active zone of the counter-vortex flow to the design section are indicated on the velocity profiles as multiples of the radius of the cylindrical channel: $x = 5R$, $10R$, $20R$, $40R$, $80R$. The flow regime is laminar; the results were obtained with $\mathrm{Re} = 500$. At the entrance to the active zone (x = 0), the following parameters have been set (Table 1).

The initial parameters listed in Table 1 cover some typical counter-vortex regimes:

- regimes of two-layer flow within the length flow energy dissipation transformed to longitudinal-axial one without swirling at a length x = 40R, Figure 2, *a, b, c*;
- the regime of the four-layer flow turns to a longitudinal-axial flow at length x = 20R, Figure 2, *d;*
- the regime with residual circulation at the exit from the active zone (x = 40R) towards more powerful peripheral or internal eddies, Figure 2, *e, f.*

Table 1. Parameters of counter-vortex flow at initial section (x=0)

Sl.No.	Initial circulation Γ_0	Angular movement velocity, Ω_0	Rossby number, Ro*	μ value	Figure
1	-1.1	3.8	0.0	-	Figure 2, a
2	0.0	0.0	1.0	6.6	Figure 2, b
3	-0.5	2.0	0.6	6.6	Figure 2, c
4	0.0	0.0	0.8	13.0	Figure 2, d
5	0.0	2.5	0.8	6.6	Figure 2, e
6	-0.5	0.0	0.0	6.6	Figure 2, f

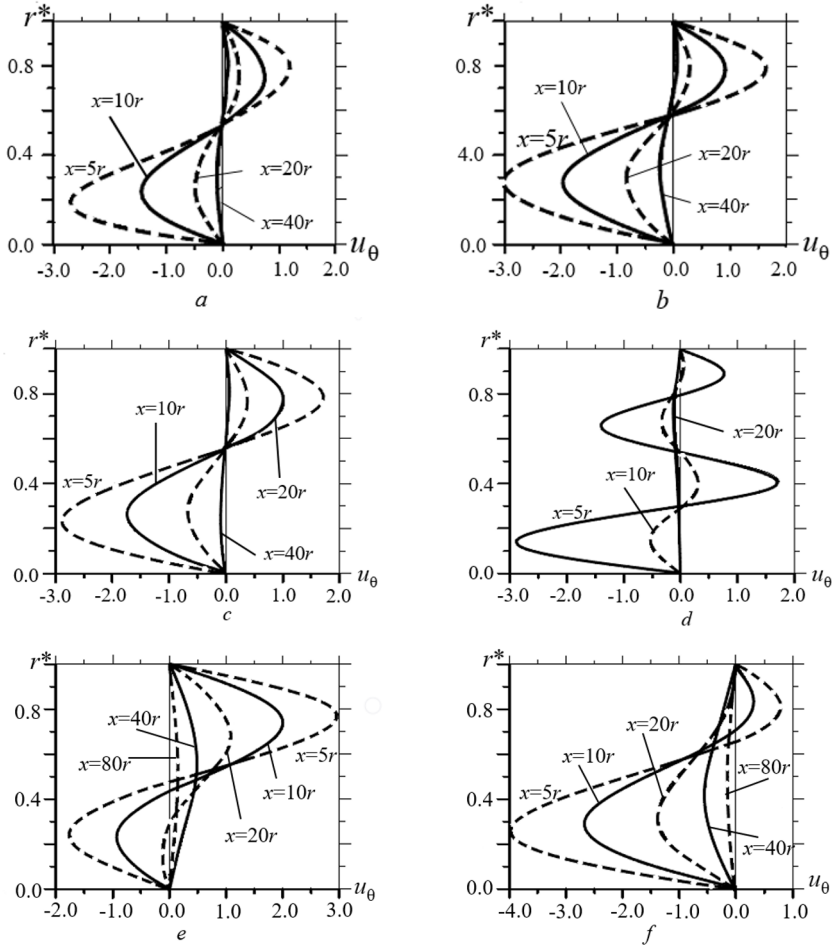

Fig. 2. Distributions of circumferential components of total velocity in counter-vortex flow as function of r^*, u_θ, x, laminar flow regime

Let us consider the results obtained on a physical model. A local swirler installed on the model has formed the initial conditions of the counter-vortex flow following item 1 of Table 1. Figure 3 shows the peripheral velocity profiles. It can be seen that the length of the active zone (interaction zone) has significantly reduced in turbulent flow. The complete

degeneration of the circulation of the counter-vortex flow is observed at a length of 11.7 radii of a circular cylindrical chamber of the interaction of oppositely rotating layers of the fluid. The longitudinal-axial Poiseuille flow is observed here with $x > 11.7R$.

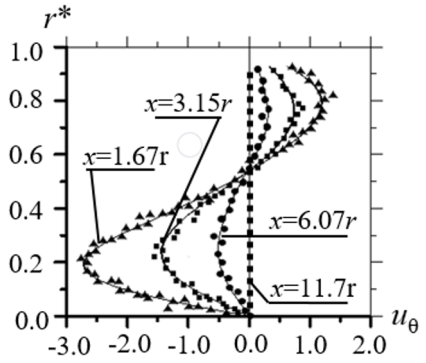

Fig. 3 Distribution of circumferential components of total velocity in counter-vortex flow as function of r^*, u_θ, x turbulent flow regime.

As to the configuration of the profiles in the cross-sections of the tube flow conductor, we can say that they quite closely coincide with the profiles shown in Figure 2, *a.* It should be noted here that the envelope lines of the profiles obtained on the physical model and shown in Figure 3 do not completely reach the walls of the flow conductor of the active flow zone to ($r^* = 1.0$). This is since it was impossible to obtain the flow velocity value in the near-wall area. In this area, there is a strong decrease in the angles of refraction due to the tube's curvature. Information received by video cameras is distorted.

The physical experiment showed that the turbulent flow regime practically does not affect the distribution of velocities over the cross-section of a circular chamber of the interaction of fluid layers but makes a significant correction in the length of the active zone of interaction of oppositely rotating layers towards its contraction.

The viscosity of the medium has a great influence on the diffusion of circulation in the counter-vortex flow. Let's return to expression (18). Here, the viscosity is present in the Re number. The change in viscosity has an inversely proportional effect on the length of the active zone of interaction of the fluid layers. The increase in viscosity leads to shrinkage of the active zone; with the decrease, the length of the active zone increases proportionally. It should be noted here that when calculating the turbulent circulation-longitudinal fluid flows, good convergence with experimental data is obtained using the turbulent analog of the Reynolds number

$$\mathrm{Re}_t = \frac{VR}{\varepsilon_t} = \frac{1}{\chi}\sqrt{\frac{8}{\lambda}}, \tag{20}$$

where ε_t is eddy viscosity, λ is hydraulic resistance factor along the length, $\chi = 0.2$ is universal constant.

In the prototype, the factor λ varies within 0.015-0.035, while the turbulent number will lie approximately in the range of $\mathrm{Re}_t = 8-135$. In the case of counter-vortex interaction of turbulent swirling flows, the length of the active zone will be reduced by about 3.5-6 times and will be in the range of length x = (7-11)R, which was shown by the comparison of calculations in the laminar regime and the data of the physical experiment in the turbulent regime.

5 Conclusions

An artificial counter-vortex flow is created by oppositely rotating fluid or gas flows. The data obtained show that the active zone of interaction between the layers decays rather quickly and turns into a longitudinal-axial flow, that is, a flow without swirling. The results of analytical calculations based on a mathematical model for laminar flow regimes show that the length of the active zone with Re = 500 and a two-layer layout of the total flow is about 40 radii of the flow conductor of a circular channel. At this length, the intensive diffusion of the initial circulation of interacting layers occurs due to its damping by the forces of viscosity. With an increase in the number of interacting layers from 2 to 4, the diffusion length decreases twice. Creating an initial imbalance in the angular momentum of the interacting layers does not lead to a change in the diffusion length of circulation.

A comparison of the results obtained on the physical model in the turbulent regime with the data of the laminar flow shows that the configuration of the profiles of the circumferential components of the counter-vortex flow velocities practically coincides. In this case, the length of the active zone of interaction of fluid layers (two-layer flow) greatly decreases from 40 to 11.7 channel radii. Thus, the flow pattern significantly affects the length of the counter-vortex flow.

Introducing the turbulent Reynolds number instead of the usual Re_t e into the analytical expression for the peripheral velocity u_θ makes it possible to obtain results close to real flow conditions. This circumstance provides the basis for applying analytical calculations to obtain the kinematics of the counter-vortex flow with preliminary estimations of the parameters of hydraulic structures in the prototype.

References

1. B. Ghazi, R. Daneshfaraz, E. Jeihouni, J. of Groundwater Science and Engineering, **7**(4), (2019)
2. M. Cihan Aydin, J. of Hydraulic Eng. **24**, (2018)
3. J. Lian, X. Wang, W. Zhang, B. Ma, D. Liu, International J. of Environmental Research and Public Health, **14**(12), (2017)
4. P. Gadge, V. Jothiprakash, V. Bhosekar, J. of Applied Water Engineering and Research, **6**(2), (2018)
5. J. Toro, F. Bombardelli, J. Paik, I. Meireles, A. Amador, Environmental Fluid Mechanics **16**(6), (2016)
6. J.-H. WU, L. YAO, F. MA, W.-W. WU, J. of Hydrodynamics, **26**, (2014)
7. M. Fathi-Moghadam, S. Kiani, P. Asiaban, R. Behrozi-Rad, International J. of Civil Engineering, **15**(4), (2017)
8. G. Orekhov, IOP Conference Series: Materials Science and Engineering, **365**(4),042023, (2018)
9. P. Gadge, V. Jothiprakash, V. Bhosekar, ISH J. of Hydraulic Engineering, **25**(1), (2019)
10. J.-H. Wu, S.-F. Li, F. Ma, J. of Hydrodynamics, **30**(2), (2018)
11. N. Fehn, D. Kozlov, I. Rumyancev, Power Techn. and Engin. **8**, (2015)
12. I. Sliva, G. Lapin, Power Techn. and Engin., **11**, (2017)
13. J. Nan, Z. Niu, Yingyong Lixue Xuebao/Chinese J. of Applied Mechanics, **35**(2), (2018)
14. J. Nan, Z. Niu, D. Hong, J. Zhu, X. Wu, Shuili Fadian Xuebao, J. of Hydroelectric Engineering, **32**(3), (2013)
15. H. Hashimoto, J. of Fluids Engineering, Transactions of the ASME, **93**(1) (1971)
16. A. Zuikov, G. Orekhov, T. Suehtina, MATEC Web of Conferences, **193**,**02024**, (2018)

17. D. Xiaotang, X. Dalei, Z. Feng, Z. Hui, Y. Cun, Proceedings of 2015 7th International Conference on Modelling, Identification and Control, ICMIC 2015, **7409372** (2016)
18. G. Orekhov, E3S Web of Conferences, **97**,**05051**, (2019)
19. G. Orekhov, OP Conference Series: Materials Science and Engineering, **869**(7), **072055** (2020)
20. V. Volshanik, V. Karelin, A. Zuikov, G. Orekhov, Hydrotechnical Construction J., **34**(11), (2000)
21. W. Yang, J. Pu, J. Wang, J. of Turbomachinery, **138**(11), (2016)
22. E. Darvishi, J.D. Fenton, S. Kouchakzadeh, J. of Hydraulic Research, **55**(3), (2017)